Extension of Kelvin's Minimum Energy Theorem to Flows with Open Regions

Tony Saad* and Joseph Majdalani†
University of Tennessee Space Institute, Tullahoma, TN 37388, USA

Kelvin's minimum energy theorem predicts that the irrotational motion of a homogenously incompressible fluid in a simply connected region will carry less kinetic energy than any other profile that shares the same normal velocity conditions on the domain's boundary. In this work, Kelvin's analysis is extended to regions with open boundaries on which the normal velocity requirements are relaxed. Given the ubiquity of practical configurations in which open regions arise, it may be argued that the longstanding question of whether Kelvin's theorem will continue to hold remains of fundamental interest. In reconstructing Kelvin's proof, we find it useful to denote a Kelvin surface as a boundary along which the net normal rotational velocity vanishes. The net rotational velocity refers to the difference between the generally rotational mean flow and the corresponding potential motion. Along similar lines, the term open is used to define a boundary along which Kelvin's velocity requirement is not fulfilled. After some analysis, two criteria are obtained, one being sufficient but not necessary, that ensure the validity of Kelvin's theorem. Both require the evaluation of a simple surface integral over the open boundary. Specific cases are then considered to illustrate the applicability of these criteria and test their usefulness. These include a variety of classic problems involving Poiseuille flow in a duct, Taylor flow in a porous channel, Taylor-Culick flow in a porous cylinder, and bidirectional helical flows of both complex lamellar and Beltramian types that may occur in a cylindrical chamber.

Nomenclature

$\boldsymbol{n}$	=	outward pointing normal unit vector
r	=	radial coordinate (cylindrical)
$\mathcal{S}$	=	surface bounding volume of fluid
$\mathcal{S}_\mathrm{K}$	=	Kelvin surface
$\mathcal{S}_\mathrm{o}$	=	open surface
T	=	specific kinetic energy of rotational motion
$\bar{T}$	=	specific kinetic energy of irrotational motion
$\boldsymbol{u}$	=	velocity field
$\bar{\boldsymbol{u}}$	=	irrotational velocity field
$\tilde{\boldsymbol{u}}$	=	vortical component of motion, $\boldsymbol{u} - \bar{\boldsymbol{u}}$
$\mathcal{V}$	=	volume of fluid
x, z	=	axial coordinate (planar and cylindrical)
y	=	normal/transverse coordinate (planar)

Greek Symbols

β	=	radial position of the mantle inside a cyclone
ϕ	=	velocity potential
ψ	=	stream function

*Graduate Research Assistant, Mechanical, Aerospace and Biomedical Engineering Department. Currently Post Doctoral Fellow, Institute for Clean and Secure Energy, University of Utah. Member AIAA.
†H. H. Arnold Chair of Excellence in Advanced Propulsion, Mechanical, Aerospace and Biomedical Engineering Department. Senior Member AIAA. Fellow ASME.

I. Introduction

Kelvin's theorems occupy a central role in understanding the motion of ideal fluids as they help to establish basic connections between purely irrotational velocity potentials and highly rotational fields. Being relevant to both classical and quantum fluids, they continue to receive attention in various fundamental studies such as those pertaining to turbulence[1,2] and aerodynamic lift.[3] Other interesting applications include a generalization of the minimum energy theorem to equivorticity flows[4] and the use of variational theory to find the conditions for minimizing the kinetic energy of vortex motions.[5] Of the many rich contributions attributed to Kelvin, the present work focuses on the minimum energy theorem. Devised in 1849, this theorem states that *the irrotational motion $\bar{\boldsymbol{u}}$ of an incompressible fluid in a simply connected region contains less kinetic energy than any other motion $\boldsymbol{u}$ with the same normal velocity at its boundary*, $\bar{\boldsymbol{u}} \cdot \boldsymbol{n} = \boldsymbol{u} \cdot \boldsymbol{n}$.[6] The additional caveat is that, for a fluid extending to infinity, the theorem requires a vanishing normal velocity at the far-field boundary.[7,8]

Several direct consequences may be deduced from Kelvin's theorem. First, it precludes the onset of irrotational motion in a simply connected, non-deformable region with rigid walls that nullify the potential velocity at all points on the boundary. Such a scenario is consistent with a system at rest or one with no kinetic energy. Second, for a non-deformable region with fixed rigid walls, no irrotational motion may be sustained when the velocity at infinity vanishes. Third, when the velocity at infinity is either null or uniform, a unique irrotational solution may be associated with a given motion of the internal boundary.[9] From this perspective, we define a Kelvin boundary as a surface on which the normal velocity requirement associated with Kelvin's theorem is satisfied, i.e. $(\bar{\boldsymbol{u}} - \boldsymbol{u}) \cdot \boldsymbol{n} = 0$. For any other boundary, the term 'open' is used. In this work, we find that Kelvin's minimum energy theorem continues to hold in regions with open boundaries provided that a simple criterion is met. This criterion will be rigourously derived and then thoroughly tested using several classic flow configurations with open boundaries.

II. Basic Analysis

In what follows, we assume that the irrotational motion can be uniquely determined given the necessary constraints. We also assume that the rotational velocity fields are incompressible and regular.

Theorem. *The irrotational motion $\bar{\boldsymbol{u}}$ of a steady homogenous incompressible fluid in a simply connected fluid region $\mathcal{V}$ contains less kinetic energy than any other motion $\boldsymbol{u}$ with or without the same normal velocity at its boundary provided that the following sufficient condition is met*

$$T_{\mathrm{o}} = \iint_{\mathcal{S}_{\mathrm{o}}} \phi \, \tilde{\boldsymbol{u}} \cdot \boldsymbol{n} \, \mathrm{d}\mathcal{S} \geq 0 \tag{1}$$

where $\tilde{\boldsymbol{u}} = \boldsymbol{u} - \bar{\boldsymbol{u}}$ defines the purely rotational component of the motion whereas ϕ, $\boldsymbol{n}$, and $\mathcal{S}_{\mathrm{o}}$ denote the velocity potential, normal unit vector, and open surface, respectively.

Proof. With $\bar{\boldsymbol{u}} = \nabla\phi$ being a steady, single-valued velocity potential of a homogeneously incompressible fluid occupying a simply connected volume of fluid $\mathcal{V}$, then $\tilde{\boldsymbol{u}} = \boldsymbol{u} - \bar{\boldsymbol{u}}$ refers to the (net) rotational contribution and difference between the velocity of another (rotational) motion satisfying continuity and the potential solution $\bar{\boldsymbol{u}}$ (see Fig. 1). Note that the rotational motion can be either inviscid or viscous. These fields are incompressible and so, by virtue of mass conservation, one may put

$$\nabla \cdot \bar{\boldsymbol{u}} = \nabla \cdot \boldsymbol{u} = \nabla \cdot \tilde{\boldsymbol{u}} = 0. \tag{2}$$

Pursuant to Kelvin's argument, $\boldsymbol{u}$ and $\bar{\boldsymbol{u}}$ must exhibit the same normal velocity along the boundary of $\mathcal{V}$ or else vanish, thus defining a Kelvin surface. Using $\mathcal{S}$ to denote a surface that envelops the fluid, one may seek a more general case by decomposing $\mathcal{S}$ into

$$\mathcal{S} = \mathcal{S}_{\mathrm{K}} + \mathcal{S}_{\mathrm{o}} \tag{3}$$

where $\mathcal{S}_{\mathrm{K}}$ and $\mathcal{S}_{\mathrm{o}}$ represent the Kelvin and open surfaces, respectively. Velocity constraints at the boundaries include

$$\begin{cases} \mathcal{S}_{\mathrm{K}}: \; \tilde{\boldsymbol{u}} \cdot \boldsymbol{n} = (\boldsymbol{u} - \nabla\phi) \cdot \boldsymbol{n} = 0 \\ \mathcal{S}_{\mathrm{o}}: \; \tilde{\boldsymbol{u}} \cdot \boldsymbol{n} \neq \boldsymbol{u} \cdot \boldsymbol{n} \neq 0. \end{cases} \tag{4}$$

It may be realized that, as a consequence of the surface decomposition, the mass flowrates of both irrotational and rotational motions must be equal at the open surface. This can be seen by first putting

$$\iint_{\mathcal{S}} \tilde{\boldsymbol{u}} \cdot \boldsymbol{n} \,\mathrm{d}\mathcal{S} = \iint_{\mathcal{S}_{\mathrm{K}}} \tilde{\boldsymbol{u}} \cdot \boldsymbol{n} \,\mathrm{d}\mathcal{S} + \iint_{\mathcal{S}_{\mathrm{o}}} \tilde{\boldsymbol{u}} \cdot \boldsymbol{n} \,\mathrm{d}\mathcal{S} = 0 \tag{5}$$

then, recalling that $\tilde{\boldsymbol{u}} \cdot \boldsymbol{n} = 0$ on $\mathcal{S}_{\mathrm{K}}$, we have

$$\iint_{\mathcal{S}_{\mathrm{o}}} \tilde{\boldsymbol{u}} \cdot \boldsymbol{n} \,\mathrm{d}\mathcal{S} = 0 \tag{6}$$

which leaves us with the equal flux requirement,

$$\iint_{\mathcal{S}_{\mathrm{o}}} \boldsymbol{u} \cdot \boldsymbol{n} \,\mathrm{d}\mathcal{S} = \iint_{\mathcal{S}_{\mathrm{o}}} \bar{\boldsymbol{u}} \cdot \boldsymbol{n} \,\mathrm{d}\mathcal{S}. \tag{7}$$

Clearly, Eq. (7) is a statement of conservation of mass that links the incompressible rotational and irrotational motions. Subsequently, when the boundary conditions arising in a given problem are not sufficient for securing a unique velocity potential, Eq. (7) may be used to achieve closure. The mass equiflux requirement is also consistent with the concept of identifying and comparing fluid motions that exhibit different kinetic energies under similar conditions at the boundaries.

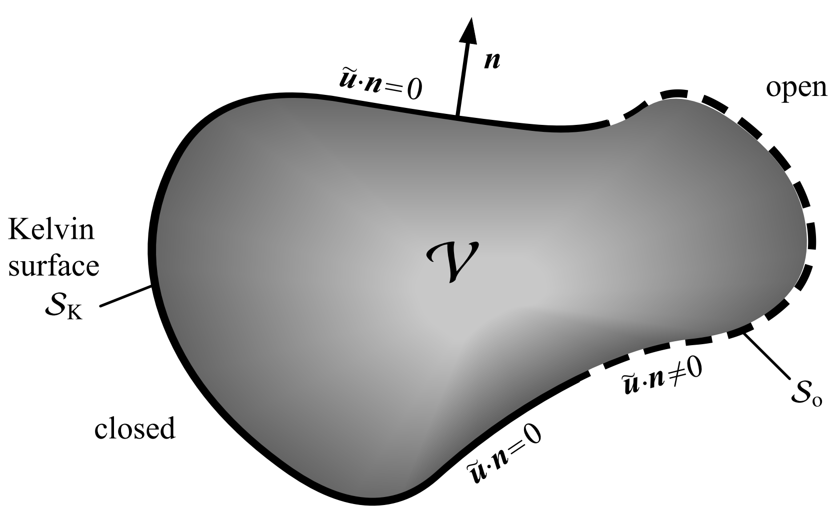

Figure 1. Volume of fluid showing both Kelvin and open surfaces with corresponding velocity requirements at the boundaries.

For steady, homogeneous, incompressible motion, we choose T and $\bar{T}$ to represent the specific kinetic energies associated with $\boldsymbol{u}$ and $\bar{\boldsymbol{u}}$, respectively. Subsequently, the energy contribution due to rotationality may be calculated from

$$\Delta T = T - \bar{T} = \tfrac{1}{2}\iiint_{\mathcal{V}} \left(\boldsymbol{u}^2 - \bar{\boldsymbol{u}}^2\right) \mathrm{d}\mathcal{V} = \tfrac{1}{2}\iiint_{\mathcal{V}} \left[(\boldsymbol{u} - \bar{\boldsymbol{u}})^2 + 2(\boldsymbol{u} - \bar{\boldsymbol{u}}) \cdot \bar{\boldsymbol{u}}\right] \mathrm{d}\mathcal{V}. \tag{8}$$

Consequently, using $\tilde{\boldsymbol{u}} \cdot \nabla\phi = \nabla \cdot (\phi\,\tilde{\boldsymbol{u}}) - \phi\nabla \cdot \tilde{\boldsymbol{u}} = \nabla \cdot (\phi\tilde{\boldsymbol{u}})$ in conjunction with the divergence theorem, Eq. (8) becomes

$$\Delta T = \widetilde{T} + T_{\mathcal{S}}; \quad \begin{cases} \widetilde{T} = \tfrac{1}{2}\iiint_{\mathcal{V}} \tilde{\boldsymbol{u}}^2\, \mathrm{d}\mathcal{V} \\ T_{\mathcal{S}} = \iint_{\mathcal{S}} \phi\, \tilde{\boldsymbol{u}} \cdot \boldsymbol{n}\, \mathrm{d}\mathcal{S}. \end{cases} \tag{9}$$

In constructing Kelvin's theorem, the purely rotational motion vanishes on all boundaries, thus yielding $\tilde{\boldsymbol{u}} \cdot \boldsymbol{n} = 0$ on $\mathcal{S}$. This permits setting $T_{\mathcal{S}} = 0$ in Eq. (9) and deducing that $\Delta T \geq 0$ with $\widetilde{T} \geq 0$ for any rotational field. It can therefore be seen that taking $\mathcal{S}$ to be a Kelvin surface ensures that the energy associated with the potential motion remains a minimum. However, in the presence of an open boundary, it is possible for $T_{\mathcal{S}} \neq 0$ granted that

$$T_{\mathcal{S}} = \iint_{\mathcal{S}_{\mathrm{K}}} \phi\, \tilde{\boldsymbol{u}} \cdot \boldsymbol{n}\, \mathrm{d}\mathcal{S} + \iint_{\mathcal{S}_{\mathrm{o}}} \phi\, \tilde{\boldsymbol{u}} \cdot \boldsymbol{n}\, \mathrm{d}\mathcal{S} = \iint_{\mathcal{S}_{\mathrm{o}}} \phi\, \tilde{\boldsymbol{u}} \cdot \boldsymbol{n}\, \mathrm{d}\mathcal{S}. \tag{10}$$

The rotational energy increment becomes

$$\Delta T = \tfrac{1}{2}\iiint_{\mathcal{V}} \tilde{\boldsymbol{u}}^2\, \mathrm{d}\mathcal{V} + \iint_{\mathcal{S}_{\mathrm{o}}} \phi\, \tilde{\boldsymbol{u}} \cdot \boldsymbol{n}\, \mathrm{d}\mathcal{S}. \tag{11}$$

Clearly, in order for $\Delta T \geq 0$, it is necessary and sufficient to impose

$$\tfrac{1}{2}\iiint_{\mathcal{V}} \tilde{\boldsymbol{u}}^2\, \mathrm{d}\mathcal{V} + \iint_{\mathcal{S}_{\mathrm{o}}} \phi\, \tilde{\boldsymbol{u}} \cdot \boldsymbol{n}\, \mathrm{d}\mathcal{S} \geq 0. \tag{12}$$

Recalling that the first term in Eq. (12) is always positive, it is sufficient although not necessary to show that

$$T_{\mathrm{o}} \equiv \iint_{\mathcal{S}_{\mathrm{o}}} \phi\, \tilde{\boldsymbol{u}} \cdot \boldsymbol{n}\, \mathrm{d}\mathcal{S} \geq 0. \tag{13}$$

Kelvin's theorem may thus be extended to the flow of homogeneously incompressible fluids in regions with open boundaries when either of the two above conditions is fulfilled. These may be implemented in the following rational order

$$\begin{cases} T_{\mathrm{o}} = \iint_{\mathcal{S}_{\mathrm{o}}} \phi\, \tilde{\boldsymbol{u}} \cdot \boldsymbol{n}\, \mathrm{d}\mathcal{S} \geq 0 & \text{(a)} \\ \text{else, if} \quad T_{\mathrm{o}} < 0, & \\ T_{\mathrm{o}} > -\tfrac{1}{2}\iiint_{\mathcal{V}} \tilde{\boldsymbol{u}}^2\, \mathrm{d}\mathcal{V} & \text{(b).} \end{cases} \tag{14}$$

□

Evidently, it is simpler to evaluate Eq. (14a), being a local surface integral, than Eq. (14b), which involves a triple integral of the net rotational velocity over the entire fluid domain.

Before leaving this topic, it may be instructive to note that the criteria established in Eq. (14) were first considered by the authors in a study that was centered on the Lagrangian optimization of wall-injected flows in porous ducts.[10] Therein, the authors applied a variational principle for the purpose of identifying classes of solutions for porous duct flows with varying energy signatures and vorticity distributions. In the process, Kelvin's extended theorem was invoked to confirm the irrotational nature of the minimum energy profile predicted by the optimization procedure. Here, the theorem is reconstructed in the light of original new applications and essential concepts such as: (a) the character of the domain boundary decomposition, (b) the specification of a Kelvin surface in Eq. (3) for denoting the closed section of the boundary, and (c) the identification of the mass equiflux condition in Eq. (7) as a basic requirement for achieving closure in the determination of unique velocity potentials (e.g. in the treatment of problems lacking sufficient boundary conditions on the irrotational motion). Finally, the present investigation will lead to the development of several potential flow representations for a rich class of helical flows[11–16] that will be described below.

III. Discussion

For a multi-valued potential such as that corresponding to the flow in multiply connected regions, the theorem no longer holds unless one selects the particular irrotational motion that bears the least kinetic energy among all potential solutions. Alternatively, if one defines a velocity potential as the difference between two possible potential solutions having the same cyclic constant ($\phi = \phi_0 - \phi_1$), then the theorem will be true owing to the resulting potential becoming unique.[8]

Since velocity potentials are defined up to an additive constant K, its effect on Eq. (14a) must be carefully examined. In this case, we replace ϕ by $(\phi + K)$ in Eq. (14a) and recover

$$T_{\mathrm{o}} = \iint_{\mathcal{S}_{\mathrm{o}}} (\phi + K)\,\tilde{\boldsymbol{u}} \cdot \boldsymbol{n}\,\mathrm{d}\mathcal{S} = \iint_{\mathcal{S}_{\mathrm{o}}} \phi\,\tilde{\boldsymbol{u}} \cdot \boldsymbol{n}\,\mathrm{d}\mathcal{S} \geq 0 \tag{15}$$

where the divergence-free property of the net rotational motion is employed by virtue of

$$\iint_{\mathcal{S}} \tilde{\boldsymbol{u}} \cdot \boldsymbol{n}\,\mathrm{d}\mathcal{S} = \iint_{\mathcal{S}_{\mathrm{K}}} \tilde{\boldsymbol{u}} \cdot \boldsymbol{n}\,\mathrm{d}\mathcal{S} + \iint_{\mathcal{S}_{\mathrm{o}}} \tilde{\boldsymbol{u}} \cdot \boldsymbol{n}\,\mathrm{d}\mathcal{S} = \iint_{\mathcal{S}_{\mathrm{o}}} \tilde{\boldsymbol{u}} \cdot \boldsymbol{n}\,\mathrm{d}\mathcal{S} = 0. \tag{16}$$

It can thus be seen that, for single-valued velocity potentials, the extended Kelvin criterion is not affected by the addition of an arbitrary constant to the potential.

IV. Applications

A wide array of flow problems exist on which the criteria given by Eq. (14) may be tested. Of those, we select the Poiseuille flow in a duct, the Taylor flow in a porous channel, the Taylor-Culick flow in a porous cylinder, and the bidirectional vortex in a confined cylinder with both complex lamellar and Beltramian motions, respectively.

A. Poiseuille Flow in Ducts of Arbitrary Cross-Sections

For this classical problem, the velocity potential corresponds to that of a uniform planar flow such that the velocity remains parallel to the duct walls. Being axially independent, the potential and rotational velocity fields return the same difference at any cross-section of the duct i.e. $\tilde{\boldsymbol{u}} \neq \tilde{\boldsymbol{u}}(z)$. Then, having single inlets and outlets as open boundaries, we easily deduce that

$$T_{\mathrm{o}} = \iint\limits_{\mathcal{S}_{\mathrm{o}}} \phi\tilde{\boldsymbol{u}} \cdot \boldsymbol{n}\,\mathrm{d}\mathcal{S} = \iint\limits_{\mathcal{S}_{\mathrm{inlet}}} \phi\tilde{\boldsymbol{u}} \cdot \boldsymbol{n}\,\mathrm{d}\mathcal{S} - \iint\limits_{\mathcal{S}_{\mathrm{outlet}}} \phi\tilde{\boldsymbol{u}} \cdot \boldsymbol{n}\,\mathrm{d}\mathcal{S} = 0 \tag{17}$$

which clearly meets the lower limit of the inequality given by Eq. (14)a. By way of illustration, we select the parabolic Hagen-Poiseuille flow in a circular pipe of unit radius. This profile exhibits the known potential and rotational fields, specifically

$$\phi = U_{\mathrm{av}} z = \tfrac{1}{2} z; \quad \bar{\boldsymbol{u}} = \tfrac{1}{2}\boldsymbol{e}_z; \quad \boldsymbol{u} = (1 - r^2)\boldsymbol{e}_z \tag{18}$$

where z refers to the axial position along the pipe. The constant U_{av} in the velocity potential is obtained by applying mass conservation at an arbitrary cross-section of the pipe. The net rotational field is then obtained by taking the difference between the rotational and irrotational fields,

$$\tilde{\boldsymbol{u}} = (\tfrac{1}{2} - r^2)\boldsymbol{e}_z. \tag{19}$$

Since both the velocity potential and net rotational motion are independent of the axial location z, the inlet and outlet sections can be arbitrarily chosen. At the outset, evaluating Eq. (14a), we recover

$$\begin{aligned} T_{\mathrm{o}} &= \iint\limits_{\mathcal{S}_{\mathrm{inlet}}} \phi\, \tilde{\boldsymbol{u}} \cdot \boldsymbol{n}\, \mathrm{d}\mathcal{S} - \iint\limits_{\mathcal{S}_{\mathrm{outlet}}} \phi\, \tilde{\boldsymbol{u}} \cdot \boldsymbol{n}\, \mathrm{d}\mathcal{S} \\ &= 2\pi \int_0^1 \left(\tfrac{1}{2} - r^2\right) r\, \mathrm{d}r - 2\pi \int_0^1 \left(\tfrac{1}{2} - r^2\right) r\, \mathrm{d}r = 0. \end{aligned} \tag{20}$$

Other Poiseuille-like profiles in ducts of various cross-sections may be obtained from Batchelor,[8] White,[17] or Shivamoggi.[18]

B. Taylor Flow in a Porous Channel

The Taylor profile refers to the inviscid rotational flow in a uniformly porous channel with a non-injecting headwall.[19,20] First studied by Taylor,[21] the geometry consists of a channel that is horizontally bounded by $0 \le x \le L$ and vertically by $0 \le y \le 1$, as shown in Fig. 2. Being rotational, Taylor's solution satisfies the no-slip boundary condition at the injecting sidewall. In the propulsion and aeroacoustic communities, this basic model is used to study rocket internal mean flow stability,[22–24] particle-mean flow interactions,[25] compressibility effects,[26] and propellant grain regression effects.[27] It is defined by[21]

$$\psi = x \sin(\tfrac{1}{2}\pi y); \quad \boldsymbol{u} = \tfrac{1}{2}\pi x \cos\left(\tfrac{1}{2}\pi y\right)\boldsymbol{e}_x - \sin\left(\tfrac{1}{2}\pi y\right)\boldsymbol{e}_y. \tag{21}$$

The potential function for this profile stems from a power law conformal map with an exponent of 2; as such, we have

$$\phi + \mathrm{i}\psi = \tfrac{1}{2} z^2; \quad z = x + \mathrm{i}y. \tag{22}$$

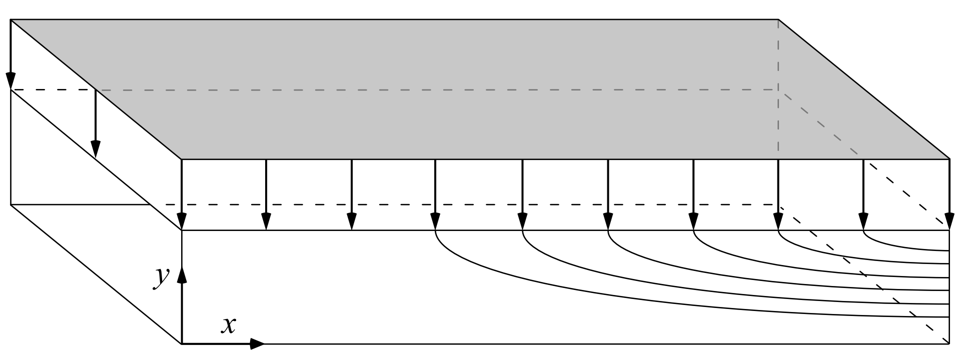

Figure 2. Streamlines corresponding to Taylor's flow in a porous channel of unit height and length L.

The corresponding velocity potential, streamfunction, and velocity field may be expressed as

$$\phi = \tfrac{1}{2}(x^2 - y^2); \quad \psi = xy; \quad \bar{\boldsymbol{u}} = x\,\boldsymbol{e}_x - y\,\boldsymbol{e}_y. \tag{23}$$

This irrotational solution may also be obtained by solving $\nabla^2\psi = 0$ with a suitable set of boundary conditions, namely,

$$\begin{cases} u(0,y) = \dfrac{\partial\psi(0,y)}{\partial y} = 0 & \text{impermeable headwall} & \text{(a)} \\ v(x,1) = -\dfrac{\partial\psi(x,1)}{\partial x} = -1 & \text{constant sidewall injection} & \text{(b)} \\ v(x,0) = -\dfrac{\partial\phi(1,z)}{\partial r} = 0 & \text{no flow across the symmetry plane} & \text{(c).} \end{cases} \tag{24}$$

With $\bar{\boldsymbol{u}}$ at hand, the net rotational component may be retrieved viz.

$$\tilde{\boldsymbol{u}} = \boldsymbol{u} - \bar{\boldsymbol{u}} = \left[\tfrac{1}{2}\pi x\cos\left(\tfrac{1}{2}\pi y\right) - x\right]\boldsymbol{e}_x + \left[y - \sin\left(\tfrac{1}{2}\pi y\right)\right]\boldsymbol{e}_y. \tag{25}$$

For the fluid domain depicted in Fig. 2, the exit plane at $z = L$ constitutes the only open boundary. Implementation of Eq. (14)a renders

$$\begin{aligned} T_\mathrm{o} &= \iint_{\mathcal{S}_\mathrm{o}} \phi\tilde{\boldsymbol{u}}\cdot\boldsymbol{n}\,\mathrm{d}\mathcal{S} = \iint_{\mathcal{S}_\mathrm{o}} (\phi\tilde{u}_x)|_{x=L}\,\mathrm{d}\mathcal{S} \\ &= \int_0^1 \tfrac{1}{2}\left(L^2 - y^2\right)\left[\tfrac{1}{2}\pi L\cos\left(\tfrac{1}{2}\pi y\right) - L\right]\mathrm{d}y = \left(4\pi^{-2} - \tfrac{1}{3}\right)L > 0. \end{aligned} \tag{26}$$

Clearly, the positive outcome ensures the validity of Kelvin's theorem. On this subject, it may be instructive to note that, in separate work, the authors[28] have applied the Lagrangian optimization principle and obtained an independent confirmation of the irrotational motion being indeed the least kinetic energy bearer among other possible flow configurations. The applicability of Kelvin's framework to an open region can hence be corroborated through the use of a fundamental principle in variational calculus.

C. Taylor-Culick Flow in a Porous Pipe

Another application of Eq. (14)a consists of the axisymmetric flow analog of Taylor's planar problem. The setting corresponds to the inviscid gaseous motion in a semi-infinite porous cylinder with an impervious headwall and uniformly distributed sidewall mass injection (see Fig. 3). This particular profile has been chosen in previous work to represent the bulk flow of an internal burning, cylindrically-shaped, solid rocket motor.[29] Chronologically, McClure, Cantrell and Hart[30] stand among the first to have used its potential mean flow in their investigative studies of the aeroacoustic field in solid rocket motors. In the spirit of improvement, their model was superseded, shortly thereafter, by Culick's rotational flow counterpart. The latter, often called Taylor-Culick's,[31] is known for being inherently consistent with the no-slip requirement at the sidewall. This may be attributed to its boundary conditions that compel the fluid to enter the chamber perpendicularly to the injecting surface.

To reproduce the irrotational solution, Taylor-Culick's velocity potential may be returned from the Laplacian of ϕ over the domain bracketed by $0 \le r \le 1$ and $0 \le z \le L$. For the sake of simplicity, the sidewall injection velocity and the radius of the chamber may be assigned unit values. The constraints that accompany the model reduce to

$$\frac{\partial\phi(0,z)}{\partial r} = 0 \quad \text{(a);} \quad \frac{\partial\phi(r,0)}{\partial z} = 0 \quad \text{(b);} \quad \frac{\partial\phi(1,z)}{\partial r} = -1 \quad \text{(c).} \tag{27}$$

At this point, the axisymmetric velocity potential may be obtained straightforwardly. We get

$$\phi = -\tfrac{1}{2}r^2 + z^2 \quad \text{or} \quad \bar{\boldsymbol{u}} = -r\boldsymbol{e}_r + 2z\boldsymbol{e}_z. \tag{28}$$

Alternatively, one may solve for the streamfunction by foreseeing that $\nabla \times \boldsymbol{u} = \boldsymbol{0}$, or

$$\frac{\partial^2 \psi}{\partial r^2} - \frac{1}{r}\frac{\partial \psi}{\partial r} + \frac{\partial^2 \psi}{\partial z^2} = 0 \tag{29}$$

where separation of variables may be readily implemented in conjunction with mass conservation to determine the constants of integration. The equivalent route yields the conjugate streamfunction

$$\psi = r^2 z. \tag{30}$$

As for the rotational solution, it may be retrieved from the vorticity transport equation assuming a linear relation between ω_θ and ψ.[29,31] One obtains

$$\psi = z\sin(\tfrac{1}{2}\pi r^2) \quad \text{or} \quad \boldsymbol{u} = -r^{-1}\sin(\tfrac{1}{2}\pi r^2)\boldsymbol{e}_r + \pi z\cos(\tfrac{1}{2}\pi r^2)\boldsymbol{e}_z. \tag{31}$$

The corresponding rotational component may be expressed as

$$\tilde{\boldsymbol{u}} = \boldsymbol{u} - \bar{\boldsymbol{u}} = \left[-r^{-1}\sin(\tfrac{1}{2}\pi r^2) + r\right]\boldsymbol{e}_r + \left[\pi z\cos(\tfrac{1}{2}\pi r^2) - 2z\right]\boldsymbol{e}_z. \tag{32}$$

When evaluated on the boundary, Eq. (32) vanishes everywhere except in the exit plane at $z = L$, where an open boundary is present. To verify that the potential solution given by Eq. (28) carries the least kinetic energy, we examine the first criterion in Eq. (14), namely,

$$\begin{aligned} T_\mathrm{o} = \iint_{\mathcal{S}_\mathrm{o}} \phi\,\tilde{\boldsymbol{u}}\cdot\boldsymbol{n}\,\mathrm{d}\mathcal{S} &= \iint_{\mathcal{S}_\mathrm{o}} (\phi\,\tilde{u}_z)_{z=L}\,\mathrm{d}\mathcal{S} \\ &= 2\pi L\int_0^1 (L^2 - \tfrac{1}{2}r^2)\left[\pi\cos(\tfrac{1}{2}\pi r^2) - 2\right] r\,\mathrm{d}r. \end{aligned} \tag{33}$$

Upon evaluation, Eq. (33) yields $T_\mathrm{o} = \left(2 - \tfrac{1}{2}\pi\right)L \geq 0$, thus ensuring $\bar{T} \leq T$. The authors have also verified that the potential solution indeed corresponds to the motion with least kinetic energy using a variational procedure based on Lagrangian multipliers.[32]

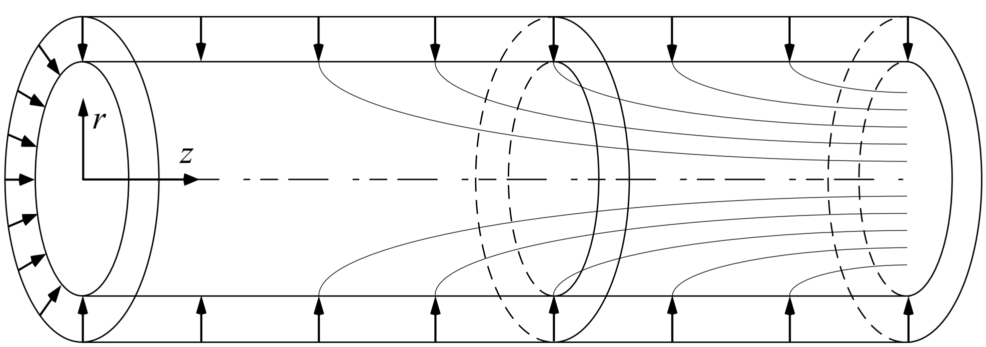

Figure 3. Streamlines corresponding to Culick's rotational profile for flow in a porous cylinder of unit radius and length L.

D. Bidirectional Vortex in a Confined Cylinder

The confined bidirectional vortex is illustrated schematically in Fig. 4. It pertains to the bipolar swirling motion of an incompressible fluid in a right-cylindrical chamber of height L and unit radius. This problem has been extensively investigated by Majdalani and co-workers.[11–16] A characteristic of the bidirectional vortex is the presence of a rotating fluid interface known as the mantle. This so-called spinning wheel separates the outer and inner vortex regions at a radius of $r = \beta$.[11,12] In this vein, the mantle position β denotes the locus of points along which the axial flow vanishes before switching spatial polarity.

The velocity potential for the bidirectional vortex can be determined by first splitting the domain into two regions. An inner cylinder bounded by the mantle ($0 \le r < \beta$) and an outer annulus extending from the mantle to the sidewall ($\beta < r \le 1$). Corresponding boundary conditions consist of

$$0 \le r < \beta : \begin{cases} \bar{u}_z(r,0) = 0 \\ \bar{u}_r(0,z) = 0 \end{cases} \qquad \beta < r \le 1 : \begin{cases} \bar{u}_z(r,0) = 0 \\ \bar{u}_r(1,z) = 0 \end{cases} \quad ; \quad \bar{u}_\theta(1,z) = 1. \tag{34}$$

Then, by using $\phi = f(r) + g(\theta) + h(z)$ in $\nabla^2\phi = 0$, one arrives at

$$\phi = \begin{cases} -\frac{1}{2}a_0 r^2 + \theta + a_0 z^2; & 0 \le r < \beta \\ -b_0(\frac{1}{2}r^2 - \ln r) + \theta + b_0 z^2; & \beta < r \le 1 \end{cases} \tag{35}$$

and so

$$\bar{\boldsymbol{u}} = \begin{cases} -a_0 r \boldsymbol{e}_r + r^{-1}\boldsymbol{e}_\theta + 2a_0 z \boldsymbol{e}_z; & 0 \le r < \beta \\ -b_0(r - r^{-1})\boldsymbol{e}_r + r^{-1}\boldsymbol{e}_\theta + 2b_0 z \boldsymbol{e}_z; & \beta < r \le 1. \end{cases} \tag{36}$$

The constants a_0 and b_0 are related by matching the inner and outer radial velocities at the mantle viz

$$b_0 = \frac{\beta^2 a_0}{\beta^2 - 1}. \tag{37}$$

While the mantle location is prescribed by the rotational motion, a_0 must be evaluated, by virtue of Eq. (7), from mass conservation at the open bounday:

$$\int_0^\beta \bar{u}_z(r,L) r dr = \int_0^\beta u_z(r,L) r dr. \tag{38}$$

In some rotational models of bidirectional vortex motions, the radial velocity is axially invariant to the extent of permitting the use of an equivalent approach for determining a_0. This can be accomplished by setting $\bar{u}_r(\beta) = u_r(\beta)$ or $a_0 = -\beta^{-1} u_r(\beta)$.

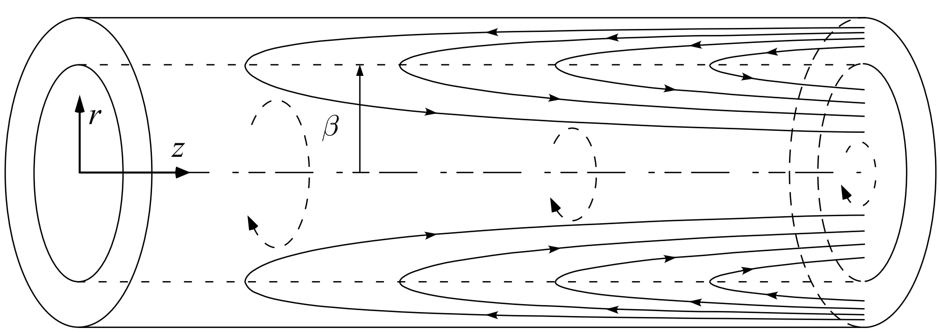

Figure 4. Schematic and coordinate system for a helical, bidirectional vortex motion in a unit- right-cylindrical chamber of length L.

At this point, Kelvin's confirmatory criteria will be applied to three models of the confined bidirectional vortex, a family of swirl dominated motions comprising three components of velocity.

1. Complex Lamellar Solution

Vyas and Majdalani[16] introduced an inviscid rotational model of the complex lamellar type for which $\boldsymbol{u} \cdot (\nabla \times \boldsymbol{u}) = 0$. Their model is summarized by

$$\boldsymbol{u} = -r^{-1} \sin(\pi r^2)\boldsymbol{e}_r + r^{-1}\boldsymbol{e}_\theta + 2\pi z \cos(\pi r^2)\boldsymbol{e}_z \tag{39}$$

where, for simplicity, we have set $\kappa = 1$ in their original solution. The mantle, in this case, is located at $\beta = 1/\sqrt{2} \simeq 0.707$. In view of Eq. (36), the net rotational component of motion may be segregated into

$$\tilde{\boldsymbol{u}} = \begin{cases} \left[2r - r^{-1}\sin(\pi r^2)\right]\boldsymbol{e}_r + \left[2\pi z\cos(\pi r^2) - 4z\right]\boldsymbol{e}_z; & 0 \le r < \sqrt{2}/2 \\ -\left[r^{-1}\sin(\pi r^2) + \left(2r - 2r^{-1}\right)\right]\boldsymbol{e}_r + \left[2\pi z\cos(\pi r^2) + 4z\right]\boldsymbol{e}_z; & \sqrt{2}/2 < r \le 1. \end{cases} \tag{40}$$

Recalling that the open boundary stands at $z = L$, Eq. (14)a may be decomposed into two complementary integrals that can be evaluated simultaneously. Using $\mathrm{Si}\,(\theta) = \int_0^\theta t^{-1}\sin t\,\mathrm{d}t$ to denote the sine integral function, this effort leads to

$$\begin{aligned} T_\mathrm{o} &= \iint\limits_{\mathcal{S}_\mathrm{o}} \phi\,\tilde{\boldsymbol{u}} \cdot \boldsymbol{n}\,\mathrm{d}\mathcal{S} = \iint\limits_{\mathcal{S}_\mathrm{o}} (\phi\,\tilde{u}_z)|_{z=L}\,\mathrm{d}\mathcal{S} \\ &= \int_0^{2\pi}\int_0^{\sqrt{2}/2}\left(2L^2 + \theta - r^2\right)\left[2\pi L\cos(\pi r^2) - 4L\right]r\,\mathrm{d}r\,\mathrm{d}\theta \\ &+ \int_0^{2\pi}\int_{\sqrt{2}/2}^{1}\left(r^2 - 2\ln r + \theta - 2L^2\right)\left[2\pi L\cos(\pi r^2) + 4L\right]r\,\mathrm{d}r\,\mathrm{d}\theta \end{aligned} \tag{41}$$

and so

$$T_\mathrm{o} = 2\left[1 - \ln 4 + \mathrm{Si}(\pi) - \mathrm{Si}\left(\tfrac{1}{2}\pi\right)\right]\pi L \simeq 0.596L > 0. \tag{42}$$

This result confirms that the complex lamellar solution is conformant to Kelvin's sufficient condition given by Eq. (14)a.

2. Beltramian Solutions

Two additional solutions of the confined bidirectional vortex have been recently reported in work by Majdalani.[11] These give rise to both Trkalian, with $\nabla \times \boldsymbol{u} = \xi\boldsymbol{u}$, $\xi = \mathrm{const}$, and Beltramian motions, with $\nabla \times \boldsymbol{u} = \xi\boldsymbol{u}$, $\xi = \xi(\boldsymbol{x})$, $\boldsymbol{x}$ being the position vector. These can be employed to substantiate Kelvin's criteria for an open region. In the interest of brevity, only the Beltramian profiles will be considered here. For this particular family, the mantle location shifts to $\beta \simeq 0.627612$, a change that affects the breakpoint in the piecewise representation of the potential field in Eqs. (35–36). As for the streamfunctions, they are compactly given by Majdalani[11] who puts them in the form

$$\psi = \begin{cases} crzJ_1(\lambda_0 r); & \text{type I} \\ cLr\sin(\tfrac{1}{2}\pi z/L)J_1(\lambda_0 r); & \text{type II} \end{cases} \tag{43}$$

where $J_1(x)$ stays for the Bessel function of the first kind, $\lambda_0 \simeq 3.83171$ is the first root of $J_1(x)$, and $c = \beta^{-1}J_1^{-1}(\lambda_0\beta) \simeq 3.069148$. While the radial and axial components of velocity are easily obtained from

Eq. (43), the tangential velocity profiles are given by

$$u_\theta = \begin{cases} r^{-1}\sqrt{1+\lambda_0^2\psi^2}; & \text{type I} \\ r^{-1}\sqrt{1+(\lambda_0^2L^2+\frac{1}{4}\pi^2)\psi^2L^{-1}}; & \text{type II.} \end{cases} \tag{44}$$

The irrotational motion is determined from Eq. (36) by setting $a_0 = 2.53874$ and $b_0 = -1.64988$ for both type I and type II solutions. In this case, evaluation of the sufficient criterion yields

$$T_\text{o} \simeq 5.163\times10^{-5}L^3 + 0.8L \ge 0; \quad \text{type I–II.} \tag{45}$$

Note that while the kinetic energy of the irrotational model is logarithmically divergent due to the presence of an irrotational vortex, it is no less singular than any of the rotational models considered. In fact, the divergent terms will cancel identically when the difference in their kinetic energies is carried out.

So while Kelvin's classic theorem remains unequivocally true in simply connected regions, the examples discussed heretofore lend support to its continued applicability to fluid domains with open regions. It is hoped that the criteria stated above will open up new lines of research inquiry, specifically ones that will either produce supplementary verifications and proofs or, perhaps, exceptions and exclusions that we may have overlooked.

V. Conclusions

The present analysis seeks to answer a long-standing question addressing the viability of Kelvin's theorem in regions with open boundaries. It seems that such a fundamental question has been judiciously avoided in textbooks on the subject, albeit relevant to a recurring problem in classical aerodynamics. Our work suggests that Kelvin's minimum energy statement is connected to the sign of an integral which, in turn, depends on the rotational flux over the open boundary and the local potential function. This no longer requires a vanishing or uniform velocity field at infinity for the theorem to stand. From this perspective, the ability of the present analysis to account for irregular velocity distributions at the fluid boundaries grants Kelvin's theorem broader applicability to geometrically complex regions and those with arbitrary velocity distributions.

Furthermore, our analysis identifies a criterion that can be invoked to secure unique velocity potentials. This additional condition ensures the equivalence of mass flowrates between irrotational motions and those with different vorticity distributions at the open boundary. By applying this principle to helical vortex motions, we are able to derive unique velocity potentials for the given boundary conditions. These motions are not only of great significance to flow separation industries, but also to propulsion, meteorology, and ocean circulation.

Finally, for all of the applications provided in this manuscript, the sufficient criterion given by Eq. (14a) held true. While the authors hope to address the universality of this condition in a future study, it represents a simple constraint to check for the minimum energy bearing motion. It is hoped that the work initiated here will be expanded to other restricted theorems, compressible fluid motions, and more elaborate physical and geometric settings.

Acknowledgments

This material is based on work supported by the National Science Foundation through Grant No. CMMI-0928762, Dr. Eduardo A. Misawa, Program Director. The authors thank Professor Jie-Zhi Wu of Peking University for his insightful comments regarding the limitations of Lord Kelvin's classic energy theorem.

References

[1]Chen, S., Eyink, G. L., Wan, M., and Xiao, Z., "Is the Kelvin Theorem Valid for High Reynolds Number Turbulence?" *Physical Review Letters*, Vol. 97, No. 14, 2006, pp. 144505–144508. doi:10.1103/PhysRevLett.97.144505.

[2]Eyink, G. L., "Cascade of Circulations in Fluid Turbulence," *Physical Review E (Statistical, Nonlinear, and Soft Matter Physics)*, Vol. 74, No. 6, 2006, pp. 066302–11. doi:10.1103/PhysRevE.74.066302.

[3]Wu, J. Z., Ma, H. Y., and Zhou, M. D., *Vorticity and Vortex Dynamics*, Springer-Verlag, New York, 2006. doi:10.1007/978-3-540-29028-5.

[4]Arnol'd, V. I., "Variational Principle for Three-Dimensional Steady-State Flows of an Ideal Fluids," *Journal of Applied Mathematics and Mechanics*, Vol. 29, No. 5, 1965, pp. 1002–1008. doi:10.1016/0021-8928(65)90119-X.

[5]Chefranov, A., and Chefranov, S., "Extrema of the Kinetic Energy and its Dissipation Rate in Vortex Flows," *Doklady Physics*, Vol. 48, No. 12, 2003, pp. 696–700. doi:10.1134/1.1639440.

[6]Thomson, W., "Notes on Hydrodynamics V: On the Vis-Viva of a Liquid in Motion," *Cambridge and Dublin Mathematical Journal*, Vol. 4, 1849, pp. 90–94.

[7]Lamb, H., *Hydrodynamics*, Cambridge University Press, Cambridge, UK, 1895.

[8]Batchelor, G. K., *An Introduction to Fluid Dynamics*, Cambridge University Press, Cambridge, UK, 1967.

[9]Rouse, H., editor, *Advanced Mechanics of Fluids*, John Wiley, New York, 1959.

[10]Saad, T., and Majdalani, J., "On the Lagrangian Optimization of Wall-Injected Flows: from the HartMcClure Potential to the TaylorCulick Rotational Motion," *Proceedings of the Royal Society of London, Series A*, Vol. 466, No. 2114, 2010, pp. 331–362. doi:10.1098/rspa.2009.0326.

[11]Majdalani, J., "Exact Eulerian Solutions of the Cylindrical Bidirectional Vortex," *45th AIAA/ASME/SAE/ASEE Joint Propulsion Conference and Exhibit*, AIAA Paper 2009-5307, Denver, Colorado, Aug. 2009.

[12]Majdalani, J., and Chiaverini, M. J., "On Steady Rotational Cyclonic Flows: The Viscous Bidirectional Vortex," *Physics of Fluids*, Vol. 21, No. 10, 2009, pp. 10360301–15. doi:10.1063/1.3247186.

[13]Maicke, B. A., and Majdalani, J., "A Constant Shear Stress Core Flow Model of the Bidirectional Vortex," *Proceedings of the Royal Society of London, Series A*, Vol. 465, No. 2103, 2009, pp. 915–935. doi:10.1098/rspa.2008.0342.

[14]Saad, T., and Majdalani, J., "Energy Based Solutions of the Bidirectional Vortex," *44th AIAA/ASME/SAE/ASEE Joint Propulsion Conference and Exhibit*, AIAA Paper 2008-4832, Hartford, Connecticut, July 2008.

[15]Majdalani, J., and Rienstra, S., "On the Bidirectional Vortex and Other Similarity Solutions in Spherical Coordinates," *Zeitschrift für Angewandte Mathematik und Physik (ZAMP)*, Vol. 58, No. 2, 2007, pp. 289–308. doi:10.1007/s00033-006-5058-y.

[16]Vyas, A., and Majdalani, J., "Exact Solution of the Bidirectional Vortex," *AIAA Journal*, Vol. 44, No. 10, 2006, pp. 2208–2216. doi:10.2514/1.14872.

[17]White, F. M., *Viscous Fluid Flow*, McGraw-Hill, New York, 3rd ed., 2005.

[18]Shivamoggi, B. K., *Theoretical Fluid Dynamics*, John Wiley, New York, 2nd ed., 1998.

[19]Banks, W. H. H., and Zaturska, M. B., "On Flow Through a Porous Annular Pipe," *Physics of Fluids*, Vol. 4, No. 6, 1992, pp. 1131–1141. doi:10.1063/1.858231.

[20]Saad, T., and Majdalani, J., "Rotational Flowfields in Porous Channels with Arbitrary Headwall Injection," *Journal of Propulsion and Power*, Vol. 25, No. 4, 2009, pp. 921–929. doi:10.2514/1.41926.

[21]Taylor, G. I., "Fluid Flow in Regions Bounded by Porous Surfaces," *Proceedings of the Royal Society, London, Series A*, Vol. 234, No. 1199, March 1956, pp. 456–475. doi:10.1098/rspa.1956.0050.

[22]Casalis, G., Avalon, G., and Pineau, J.-P., "Spatial Instability of Planar Channel Flow with Fluid Injection through Porous Walls," *Physics of Fluids*, Vol. 10, No. 10, 1998, pp. 2558–2568. doi:10.1063/1.869770.

[23]Griffond, J., and Casalis, G., "On the Nonparallel Stability of the Injection Induced Two-Dimensional Taylor Flows," *Physics of Fluids*, Vol. 13, No. 6, 2001, pp. 1635–1644. doi:10.1063/1.1367869.

[24]Griffond, J., "Receptivity and Aeroacoustic Resonance in Channels with Blowing Walls," *Physics of Fluids*, Vol. 14, No. 11, 2002, pp. 3946–3962. doi:10.1063/1.1511546.

[25]Féraille, T., and Casalis, G., "Channel Flow Induced by Wall Injection of Fluid and Particles," *Physics of Fluids*, Vol. 15, No. 2, 2003, pp. 348–360. doi:10.1063/1.1530158.

[26]Maicke, B. A., and Majdalani, J., "On the Rotational Compressible Taylor Flow in Injection-Driven Porous Chambers," *Journal of Fluid Mechanics*, Vol. 603, No. 1, 2008, pp. 391–411. doi:10.1017/S0022112008001122.

[27]Dauenhauer, E. C., and Majdalani, J., "Exact Self-Similarity Solution of the Navier–Stokes Equations for a Porous Channel with Orthogonally Moving Walls," *Physics of Fluids*, Vol. 15, No. 6, 2003, pp. 1485–1495. doi:10.1063/1.1567719.

[28]Saad, T., and Majdalani, J., "Energy Based Mean Flow Solutions for Slab Hybrid Rocket Chambers," *44th AIAA/ASME/SAE/ASEE Joint Propulsion Conference and Exhibit*, AIAA Paper 2008-5021, Hartford, Connecticut, July 2008.

[29]Majdalani, J., and Saad, T., "The Taylor–Culick profile with arbitrary headwall injection," *Physics of Fluids*, Vol. 19, No. 9, 2007, pp. 093601–10. doi:10.1063/1.2746003.

[30]McClure, F. T., Cantrell, R. H., and Hart, R. W., "Interaction Between Sound and Flow: Stability of T-Burners," *AIAA Journal*, Vol. 1, No. 3, 1963, pp. 586–590. doi:10.2514/3.54846.

[31]Culick, F. E. C., "Rotational Axisymmetric Mean Flow and Damping of Acoustic Waves in a Solid Propellant Rocket," *AIAA Journal*, Vol. 4, No. 8, 1966, pp. 1462–1464. doi:10.2514/3.3709.

[32]Majdalani, J., and Saad, T., "Energy Steepened States of the Taylor-Culick Profile," *43rd AIAA/ASME/SAE/ASEE Joint Propulsion Conference and Exhibit*, AIAA Paper 2007-5797, Cincinnati, Ohio, July 2007.